DEPARTMENT OF THE INTERIOR
UNITED STATES GEOLOGICAL SURVEY

Prepared for the
NATIONAL AERONAUTICS AND SPACE ADMINISTRATION

ATLAS OF MARS
1:5,000,000 GEOLOGIC SERIES
NOACHIS QUADRANGLE
M 5M –48/330 G, 1977
I-910 (MC-27)

Interior—Geological Survey, Reston, Va.—1977—G76221

Prepared on behalf of the Planetology Programs Office, National Aeronautics and Space Administration under contract W-13,709 in cooperation with the Department of Geological Sciences, University of Colorado (NASA grant NGR-06-003-199)

NOTES ON BASE

This is one map in a series of preliminary mosaics covering the entire surface of Mars at a nominal scale 1:5,000,000 (Batson, 1973). The major source of map data was the Mariner 9 television experiment (Masursky and others, 1970).

ADOPTED FIGURE

The figure of Mars used for the computation of the map projection is an oblate spheroid (flattening of 1/192) with an equatorial radius of 3393.4 km and a polar radius of 3375.7 km.

PROJECTION

The Lambert conformal conic projection is used for this sheet with standard parallels at 35.8° and 59.2°. A scale of 1:4,336,000 at lat 30° was chosen to match the scale at lat 30° of the adjacent Mercator projections. Longitudes increase to the west in accordance with usage of the International Astronomical Union (IAU, 1970). Latitudes are areographic (de Vaucouleurs and others, 1973).

CONTROL

Planimetric control is provided by radio-tracked positions of the spacecraft and telemetered camera-pointing angles. The first meridian passes through the crater Airy-O (latitude 5.19° S) within the crater Airy. No simple statement is possible for the precision, but local consistency is 20-40 km.

MAPPING TECHNIQUE

Selected Mariner 9 pictures were transformed to the Lambert conformal projection and assembled in a series of mosaics at 1:5,000,000.

CONTOURS

Since Mars has no seas and hence no sea level, the datum (The 0 km contour line) for altitudes is defined by a gravity field described by spherical harmonics of fourth order and fourth degree (Jordan and Lorell, 1973) combined with a 6.1 millibar atmospheric pressure surface derived from radio-occultation data (Kliore and others, 1973; Christensen, 1975). This datum is a triaxial ellipsoid with semi-major axes of A=3394.6 km, B=3393.3 km, and a semi-minor axis of C=3376.3 km. The semi-major axis A intersects the Martian surface at long 105°.

The contour lines (Wu, 1975) were compiled from Earth-based radar determinations (Downs and others, 1971; Pettengill and others, 1971) and measurements made by Mariner 9 instrumentation, including the ultraviolet spectrometer (Hord and others, 1974), infrared interferometer spectrometer (Conrath and others, 1973), and stereoscopic Mariner 9 television pictures (Wu and others, 1973).

Formal analysis of contour-line accuracy has not been made. The estimated vertical accuracy of each source of data indicates a probable error of 1-2 km.

NOMENCLATURE

All names on this sheet are approved by the International Astronomical Union (IAU, 1974).

MC-27:	Abbreviation for Mars Chart 27.
M 5M -48/330 G:	Abbreviation of Mars 1:5,000,000 series; center of sheet, 48° S latitude, 330° longitude; geologic map, G.

REFERENCES

Batson, R. M., 1973, Cartographic products from the Mariner 9 mission: Jour. Geophys. Research, v. 78, no. 20, p. 4424-4435.
Christensen, E. J., 1975, Martian topography derived from occultation, radar, spectral, and optical measurements: Jour. Geophys. Research, v. 80, no. 20, p. 2909-2913.
Conrath, B. J., Curran, R. K., Hanel, R. A., Kunde, V. G., Maguire, W. W., Pearl, J. C., Pirraglia, J., Welker, J., and Burke, T., 1973, Atmospheric and surface properties of Mars obtained by infrared spectroscopy on Mariner 9: Jour. Geophys. Research, v. 78, no. 20, p. 4267-4278.
Downs, G. S., Goldstein, R. M., Green, R. R., and Morris, G. A., 1971, Mars radar observations, a preliminary report: Science, v. 174, no. 4016, p. 1324-1327.
Hord, C. W., Simmons, K. E., and McLaughlin, L. K., 1974, Mariner 9 ultraviolet spectrometer experiment: Pressure-altitude measurements on Mars: Icarus, v. 21, no. 3, p. 292-302.
International Astronomical Union, Commission 16, 1971, Physical study of planets and satellites, *in* Proc. 14th General Assembly, 1970: Internat. Astron. Union Trans., v. XIVB, p. 128-137.
——— 1974, Physical study of planets and satellites, *in* Proc. 15th General Assembly, 1973: Internat. Astron. Union Trans., v. XVB, p. 105-108.
Jordan, J. F., and Lorell, Jack, 1973, Mariner 9, an instrument of dynamical science: Presented at AAS/AIAA Astrodynamics Conf., Vail, Colo., July 16-18, 1973.
Kliore, A. J., Fjeldbo, Gunnar, Seidel, B. L., Sykes, M. J., and Woiceshyn, P. M., 1973, S-band radio occultation measurements of the atmosphere and topography of Mars with Mariner 9: Extended mission coverage of polar and intermediate latitudes: Jour. Geophys. Research, v. 78, no. 20, p. 4331-4351.
Masursky, Harold, Batson, R. M., Borgeson, W. T., Carr, M. H., McCauley, J. F., Milton, D. J., Wildey, R. L., Wilhelms, D. E., Murray, B. C., Horowitz, N. H., Leighton, R. B., Sharp, R. V., Thompson, T. W., Briggs, G. A., Chandeysson, P., Shipley, E. N., Sagan, Carl, Pollack, J. B., Lederberg, Joshua, Levinthal, E. C., Hartmann, W. K., McCord, T. B., Smith, B. A., Davies, M. E., de Vaucouleurs, G. D., and Leovy, C. B., 1970, Television experiment for Mariner Mars 1971: Icarus, v. 12, no. 1, p. 10-45.
Pettengill, G. H., Rogers, A. E. E., and Shapiro, I. I., 1971, Martian craters and a scarp as seen by radar: Science, v. 174, no. 4016, p. 1321-1324.
de Vaucouleurs, G. D., Davies, M. E., and Sturms, F. M., Jr., 1973, The Mariner 9 areographic coordinate system: Jour. Geophys. Research, v. 78, no. 20, p. 4395-4404.
Wu, S. S. C., Schafer, F. J., Nakata, G. M., Jordan, Raymond, and Blasius, K. R., 1973, Photogrammetric evaluation of Mariner 9 photography: Jour. Geophys. Research, v. 78, no. 20, p. 4405-4410.
Wu, S. S. C., 1975, Topographic mapping of Mars: U.S. Geol. Survey Interagency Rept. 63 (in press).

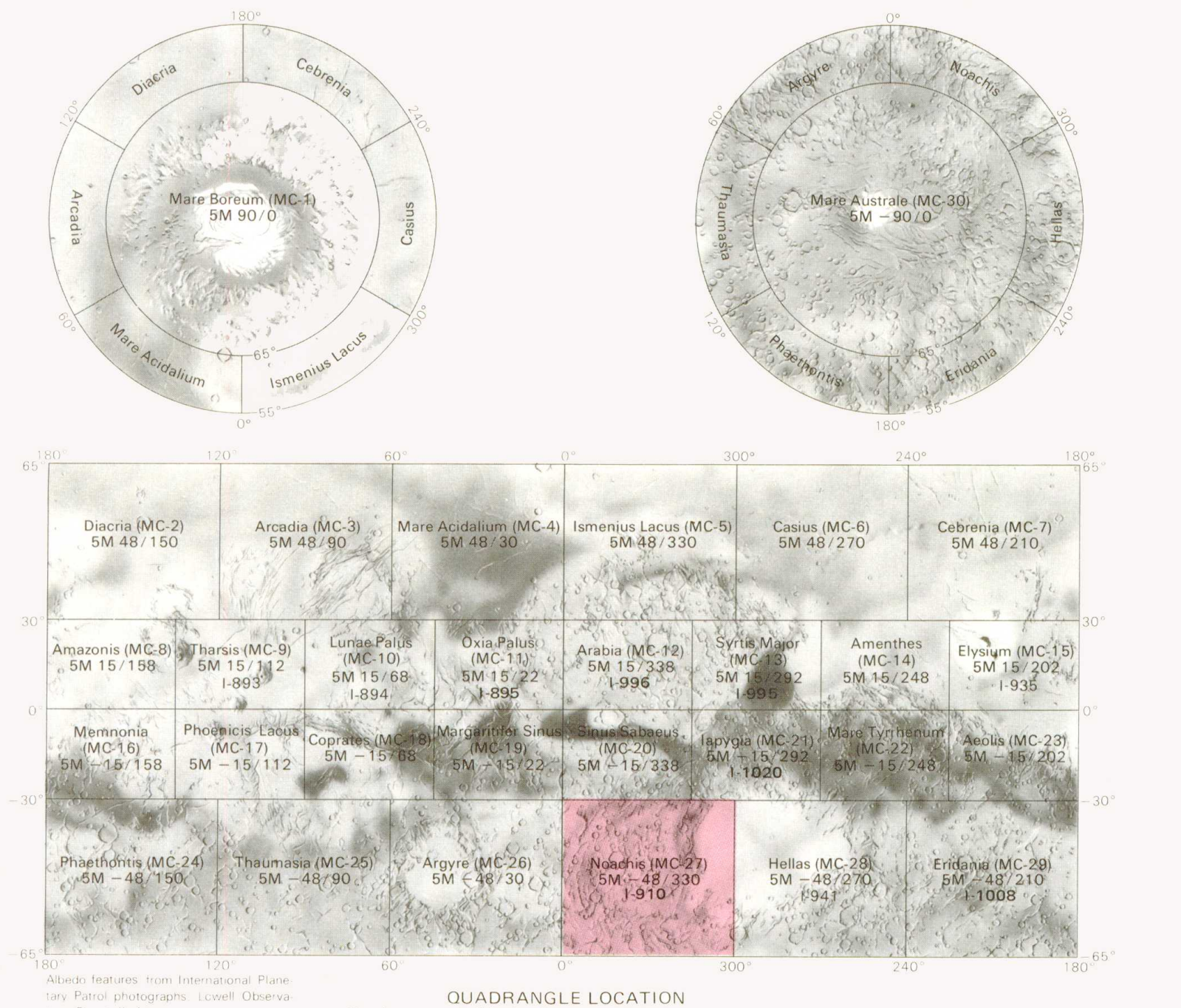

QUADRANGLE LOCATION
Number preceded by I refers to published geologic map

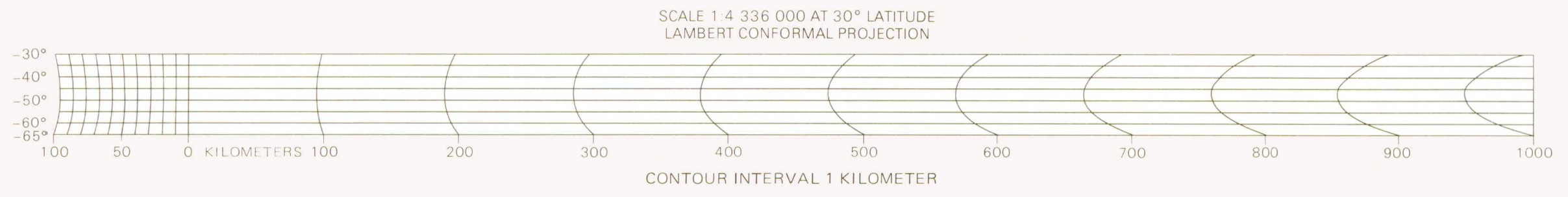

CONTOUR INTERVAL 1 KILOMETER

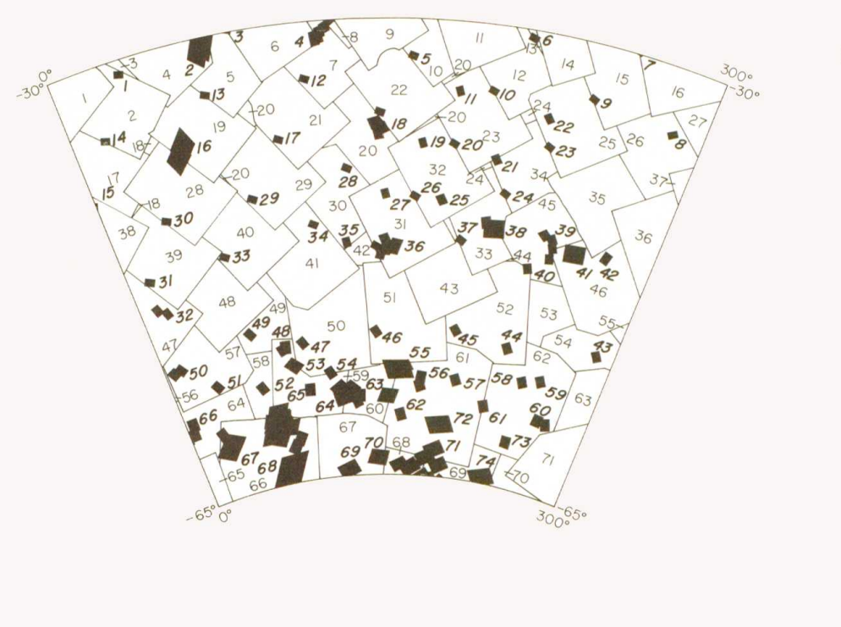

A-camera pictures

Index No.	DAS No.	Index No.	DAS No.	Index No.	DAS No.
1	8117303	25	5671153	49	5526743
2	5311283	26	5743253	50	5598703
3	5311353	27	5743323	51	5670733
4	8189269	28	5383103	52	5742763
5	5383243	29	5455063	53	5814723
6	8261229	30	5527023	54	5886683
7	5455203	31	5598983	55	5886753
8	5455278	32	5599053	56	5454643
9	8333259	33	5671013	57	5454713
10	5527233	34	5671083	58	5526673
11	8405219	35	5743183	59	5670593
12	5599193	36	5815143	60	5742623
13	5599263	37	5815213	61	5814583
14	8477249	38	5311143	62	5886613
15	5671223	39	5383033	63	5958573
16	8549279	40	5454993	64	5526603
17	5311213	41	5526953	65	5526533
18	6028578	42	5598913	66	5670523
19	5383173	43	5670943	67	5742553
20	6244388	44	6531878	68	5814513
21	5455133	45	5743113	69	5886544
22	5527163	46	5815073	70	5958503
23	5599123	47	5382963	71	6030464
24	6460058	48	5454923		

High-resolution B-camera pictures

Index No.	DAS No.	Index No.	DAS No.	Index No.	DAS No.	Index No.	DAS No.	Index No.	DAS No.
1	*5311318*	*18*	*8476794*	*36*	*9807494*	*55*	*5742658*	*68*	*6928808*
2	*5813848*		*8476864*	*37*	*5670978*	*56*	*7217418*		*6928878*
	5813918		*8476934*	*38*	*7073708*		*7217698*		*7072798*
3	*5383278*		*8477004*		*9123034*	*57*	*5814618*		*7072868*
4	*5455238*	*19*	*8404904*	*39*	*8620784*	*58*	*7289728*		*8548194*
	8332804	*20*	*5599088*		*8620854*	*59*	*5886648*		*8548264*
	8332874	*21*	*8548964*		*8620924*	*60*	*5958538*		*9735114*
	8332944	*22*	*8549034*		*8620994*		*7361408*		*10648869*
	8333014	*23*	*5671118*	*40*	*7145738*	*61*	*5886578*		*10648938*
	11620000	*24*	*5671048*	*41*	*9194924*	*62*	*5814548*	*69*	*6245538*
5	*5527198*	*25*	*8548894*	*42*	*10095544*	*63*	*10720969*	*70*	*10720899*
6	*5599228*	*26*	*5599018*	*43*	*5886718*	*64*	*5742588*	*71*	*6173718*
7	*5671258*	*27*	*8404834*	*44*	*5814688*		*7145458*		*7504348*
8	*11797031*	*28*	*5527058*	*45*	*5742728*		*7576308*		*7504628*
9	*5671189*	*29*	*5455028*	*46*	*5670698*		*8836104*		*7504698*
10	*5599158*	*30*	*5383068*	*47*	*5598668*		*8836174*		*8764144*
11	*8404974*	*31*	*5382998*	*48*	*7001398*	*65*	*7073428*		*8764214*
12	*5455168*	*32*	*6785728*		*7001678*	*66*	*5326568*		*8907574*
13	*5383208*		*6857688*	*49*	*5526708*		*6857408*		*8907644*
14	*5311248*	*33*	*5454958*	*50*	*5454678*		*6929438*		*8907714*
15	*5311178*	*34*	*5526988*		*6929718*	*67*	*5598528*		*10239114*
16	*5383138*	*35*	*8404764*	*51*	*5526638*		*7072518*		*10239184*
	7360778	*36*	*5598948*	*52*	*5598598*	*68*	*5525938*	*72*	*5130018*
	7360848		*8548824*	*53*	*11442944*		*5525868*	*73*	*7289448*
17	*5455098*		*9307424*	*54*	*5670628*		*5670558*	*74*	*5130088*
18	*5527128*		*9807354*	*55*	*5129948*		*6928528*		

INDEX TO MARINER 9 PICTURES

The mosaic used to control the positioning of features on this map was made with the Mariner 9 A-camera pictures outlined above, identified by vertical numbers. Useful coverage is not available in cross-hatched area. Also shown (by solid black rectangles) are the high-resolution B-camera pictures, identified by italic numbers. The DAS numbers may differ slightly (usually by 5) among various versions of the same picture.

GEOLOGIC MAP OF THE NOACHIS QUADRANGLE OF MARS

By
James E. Peterson
1977

CORRELATION OF MAP UNITS

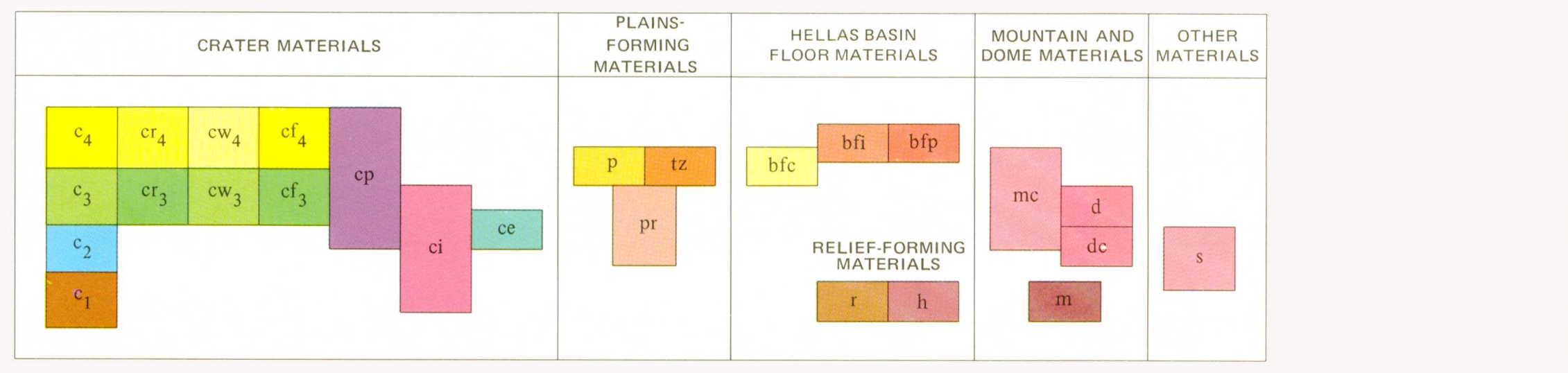

DESCRIPTION OF MAP UNITS

CRATER MATERIALS

Craters classified into four groups according to morphology and apparent relative age. The equal sizes of boxes for classes c_1 through c_4 on the correlation chart do not indicate equal time periods. Classes c_1 through c_4 interpreted as impact craters, although distinguishing characteristics lacking for classes c_1 and c_2. Craters < 20 km diameter not mapped except class c_4 craters and a few older ones that have critical relations with other features. Some large c_4 and c_3 craters subdivided into rim (cr), wall (cw), and floor (cf) materials.

c_4 CRATER MATERIAL, UNDIVIDED—Craters with sharp, elevated, complete rim crests; rough rim material extending ≥ 1 crater radius from rimcrest; steep rough walls; rough, deep floors (below adjacent terrain); with or without central peaks (cp)

cr_4 CRATER RIM MATERIAL

cw_4 CRATER WALL MATERIAL

cf_4 CRATER FLOOR MATERIAL

cp CRATER CENTRAL PEAK MATERIAL—Steep-sided peaks located at or near centers of craters. Basal diameters small relative to diameters of craters they are found in. *Interpretation:* Disrupted bedrock uplifted by impact shock-rebound

c_3 CRATER MATERIAL, UNDIVIDED—Craters with moderately sharp, elevated, complete rimcrests; texturally distinct (not rough) rim material extending < 1 crater radius from rimcrest; moderately rough, steep walls; moderately rough, deep floors (below adjacent terrain); with or without central peaks (cp)

cr_3 CRATER RIM MATERIAL

cw_3 CRATER WALL MATERIAL

cf_3 CRATER FLOOR MATERIAL

ci MATERIAL OF IRREGULARLY SHAPED CRATERS—Craters having non-circular outlines; generally with elevated rimcrests; crater rims appear to be continuous rather than a composite of over-lapping superposed craters. *Interpretation:* No common origin, probably formed by impact, volcanism or collapse

ce MATERIAL OF ELEVATED CRATERS—Craters with very high, narrow, steep rims; crater floors appear to be above level of adjacent terrain. Six occurrences in SW corner of quadrangle, one in Hellas. *Interpretation:* Origin unknown

c_2 CRATER MATERIAL—Craters with moderately subdued, slightly elevated, complete rimcrests; smooth narrow rims; moderately rough to smooth, steep to gently sloping walls; generally smooth, flat floors lower than adjacent terrain; a few with central peaks (cp). c_2 indicates rim and wall materials, undivided, or rim, wall and floor materials, undivided

c_1 CRATER MATERIAL—Craters with moderately to extremely subdued, slightly elevated to unelevated (above adjacent terrain), commonly incomplete rimcrests; smooth, narrow rims where present; smooth, steep to gently sloping walls; smooth, flat, shallow floors (at or slightly below level of adjacent terrain). c_1 indicates rim and wall materials, undivided, or rim, wall and floor materials undivided

PLAINS-FORMING MATERIALS

p PLAINS MATERIAL—Forms extensive generally smooth (at A-camera resolution) level surfaces in intercrater areas and on floors of flat-bottomed craters. B-frames show some variations in smoothness, unmappable from A-frames. Densities of craters 10 km or larger and their morphologies tend to indicate that the age of the bedrock underlying this unit is equivalent in age to older crater materials (late c_1 through early c_2). *Interpretation:* Deposits of unconsolidated surficial sediment, probably underlain by flood lavas in some areas

tz TRANSITION ZONE MATERIAL—Mapped between Hellespontus and Hellas; Similar to plains material at A-frame resolution, but appears somewhat rougher in B-frames; slopes generally downward toward Hellas; has a locally prominent system of near-parallel and en echelon ridges and scarps. Densities of craters 10 km or larger and their morphologies tend to indicate that the age of the bedrock underlying this unit is apparently equivalent in age to older crater materials (middle c_1). *Interpretation:* Colluvium, disrupted by downslope movement of surface material, underlain by faulted bedrock protruding through it as ridges and scarps

pr RIDGED PLAINS MATERIAL—Forms generally smooth, gently rolling plains south of 59° S. Contains abundant low, broad ridges, some scarps, some linear depressions, and numerous domes. *Interpretation:* Flood lavas

HELLAS BASIN FLOOR MATERIALS

bfi INTERMEDIATE BASIN-FLOOR MATERIAL—Forms abundant small (up to a few km across), nearly circular hills and generally low ridges and broad valleys running downslope between central basin floor material and peripheral basin-floor material in Hellas. *Interpretation:* Erosional slope forming at expense of central basin-floor material

bfp PERIPHERAL BASIN-FLOOR MATERIAL—Forms generally smooth (at A-frame resolution), nearly featureless plains in Hellas. Similar to plains material but very sparsely cratered. Local variations in smoothness may be caused by buried features. *Interpretation:* Deposits of unconsolidated surficial sediment

bfc CENTRAL BASIN-FLOOR MATERIAL—Forms terrain on floor of Hellas at slightly higher elevation than peripheral basin-floor material. Rough to gently rolling terrain, locally with subdued craters and scarps, all having mantled appearance. *Interpretation:* Deposits of unconsolidated surficial sediment, locally with deflation hollows, overlying bedrock of varied roughness

RELIEF-FORMING MATERIALS

r RUGGED MATERIAL—Characterized by numerous sharp ridges, scarps, and shallow depressions; generally rugged with few small smooth areas except for crater floors, which appear to be covered by plains material. *Interpretation:* Ancient bedrock, faulted and fractured, unmantled or thinly mantled by dust

h HUMMOCKY MATERIAL—Characterized by subdued hills and pits forming hummocky terrain at slightly higher elevation than adjacent terrain. Mapped only south of 60° S, except one occurrence at 35.7° S, 323° W. *Interpretation:* Remnants of ancient eroded highlands protruding through younger material

MOUNTAIN AND DOME MATERIALS

mc MATERIAL OF CRATERED MOUNTAINS—Forms steep-flanked, high-relief conical mountains with relatively small summit craters. Two occurrences mapped in Hellas basin, one with fresh smooth flanks, one (queried) highly eroded. *Interpretation:* Volcanic constructs, probably stratovolcanoes

d DOME MATERIAL—Characterized by nearly circular outlines; low, smooth, positive relief. In some places two or more domes overlap. None observed north of 59° S. *Interpretation:* Uncertain origin; may be volcanic domes and/or erosional mesas

dc MATERIALS OF CRATERED DOMES—Similar to dome material but with central craters; craters lack raised rims, are relatively wide (> ¼ dome basal diameter). Generally located on crater floors; none observed north of 57° S. *Interpretation:* Volcanic constructs, probably small shield volcanoes

m MOUNTAIN MATERIAL—Characterized by high relief, steep slopes, generally irregular outlines, and rugged appearance. Varies from small peaks (a few km across) to extensive ranges. Main occurrences in transition zone between Hellespontus and Hellas. *Interpretation:* No common origin; probably fault blocks, steptoes, and some volcanoes

OTHER MATERIALS

s SHIELD MATERIAL—Extensive, gently sloping domical mass with multiple large (>100 km diameter), subdued, shallow, rimless craters at or near the summit or summits; sparsely cratered; flanks radially lineated by narrow ridges and channels; overlaps transition zone material but contact generally indistinct. *Interpretation:* Shield volcano complex

Contact—Queried where location or existence highly uncertain

Fault—Line at crest of scarp; dashed where approximately located. Bar and ball on downthrown side. Locally serves as contact

High, steep, narrow ridge—Line at crest; dashed where approximately located. Locally serves as approximately located contact. *Interpretation:* Remnant of rotated upthrown fault block

Low, gently sloping, broad ridge—Line at crest; dashed where approximately located. Locally serves as approximately located contact. *Interpretation:* Most probably structurally controlled volcanic fissure complexes

Asymmetric ridge—Hachures on broad, gently sloping side; barb points toward steep, narrow side. Line at crest. *Interpretation:* Probably fault-controlled volcanic fissure complex with post-volcanism fault rejuvenation

Scarp—Line at crest; dashed where approximately located. Barb points downslope. Locally serves as approximately located contact. *Interpretation:* Most probably fault scarps, some possibly erosional scarps, some possibly lava-flow fronts

Trough—Narrow linear or arcuate depression. Line at bottom; dashed where approximately located. *Interpretation:* Some probably graben, some probably collapse depressions, some possibly erosional channels

Channel—Narrow sinuous depression in dendritic system. Line at bottom; dashed where approximately located. *Interpretation:* Formed by fluvial erosion

Lineament—Straight or arcuate feature of indeterminate relief. Locally serves as approximately located contact. *Interpretation:* Various origins such as fault scarps, erosional scarps and troughs, perhaps some low ridges

Circular depression—Rimless crater at summit of shield or dome. Some nearly filled. *Interpretation:* Caldera

Irregular depression—Broad, rimless. *Interpretation:* Formed by collapse

Prominent rim crest—Dashed where approximately located. Mapped only for elevated crater material and where other crater units are subdivided. Locally serves as contact

Buried rim crest—Queried where existence uncertain

Basin ring—Dotted where buried by shield. Structures including ridges, scarps, and mountains. Three Hellas rings numbered from basin center. Basin ring in northwest part of quadrangle unnumbered. *Interpretation:* Formed by faulting caused by gravitational collapse of surrounding areas toward deep initial impact crater.

Dark material—Splotches and streaks related to topography, many located on crater floors. Outlines vary from nearly circular to very irregular. *Interpretation:* Some deposits of dark eolian sediments, locally forming dune fields; some areas of dark rock exposed by deflation or nondeposition of light surficial sediments

GEOLOGIC SUMMARY

IMPACT CRATERS

The Noachis quadrangle is in the ancient cratered highlands of Mars. Craters dominate the surface of the planet in this area; most are of impact origin, some are of volcanic origin, and some are of undetermined origin.

Martian craters are in general similar in morphology to lunar craters but are more degraded. Analogous morphologies and size-frequency distributions of lunar and Martian craters indicate that both populations are mostly of impact origin (McCauley and others, 1972). Mariner 10 pictures of Mercury suggest similar trends on that planet, a further indication that the cratering process was exogenous.

Impact craters in the Noachis quadrangle are classified into four groups based on their morphologic characteristics, each group representing a relative age range. Where applicable, superposition relations support relative age determinations based on crater morphology.

Factors complicating relative age determinations include regional variations in tectonic and volcanic activity, the local presence of surficial sediments that subdue the appearances of craters and probably bury small ones, and extreme variations in image quality. Owing mainly to the presence of dust in the atmosphere, the poor quality of much of the imagery substantially hindered geologic mapping in this region, especially in the Hellas basin.

On the Moon, secondary-crater populations and stratigraphic relations of ejecta blankets with each other and with other features are useful for determining sequences of events in many areas. These criteria are much less valuable on Mars because of erosion or burial by other materials.

Central peaks are steep sided with relatively small basal diameters, and are located at the centers of craters. They are interpreted to be disrupted bedrock uplifted by shock rebound during the crater-forming process. Most Martian central-peak craters are 10 to 30 km in diameter. Central peaks are more easily eroded than crater walls, being common in young craters and nonexistent in very old craters. The irregular distribution of central-peak craters within the quadrangle is attributed to local differences in the strengths of target materials and to variations in the size, composition, and velocity of the impacting bodies.

Some craters are distinctly polygonal rather than circular, indicating that joint systems existed in the bedrock before the craters were formed.

OTHER DEPRESSIONS

Irregular craters are highly varied in their morphology and almost certainly in their origin. Some are thought to be endogenic, others exogenic. All exhibit some abnormality or ambiguous characteristics. Some (as at 38° S, 344.5° W.) are rimless, flat-floored features that can be interpreted as calderas or nonvolcanic collapse depressions. Others (as at 32° S, 328° W.) are deep, with raised rims and steep rough walls, and look like overlapping impact craters except that they lack septa.

Several large irregular depressions are mapped with a special structural symbol. Smaller ones are mapped as troughs (but most troughs appear to be grabens or channels). The lips of these depressions are sharp and the walls are steep at the top. All are closed depressions and probably formed by collapse. Some are controlled by local fracture systems.

BASINS

The western third of Hellas Planitia, the largest circular basin on Mars (about 2,000 km in diameter), occupies the eastern part of the quadrangle. Another circular basin, 400 km in diameter, is centered at 37.5° S, 356° W. It is detectable only by a low ridge or scarp around its perimeter, mapped with a special symbol. The size, circularity, and apparent old age of the basin led to the interpretation that it was created by the impact of a major body and subsequently filled by basaltic lavas (possibly interlayered with sediments), much like the lunar maria. The volcanism that filled the basin may have been triggered by the impact and probably continued into early c_3 crater time. The basin is considered to have formed very early in c_1 crater time or even pre-c_1 crater time, and probably is the oldest feature still discernible within the quadrangle.

Hellas is structurally asymmetrical, except for its general circularity. To its east is a broad marginal zone of scattered mountains not arranged in any distinct pattern clearly related to Hellas. The mountains grade into knobby terrain farther east and are interpreted by Potter (1976) to be remnants of ejecta from the Hellas basin. The transition zone to the west, which is characterized by a general slope from the high plains west of Hellespontus Montes to the floor of Hellas, contains a prominent system of subparallel ridges and scarps concentric about Hellas. These ridges and scarps are thought to be the products of normal faulting resulting from regional extension, an interpretation consistent with either an impact or a tectonic subsidence model of basin formation. The ridges and scarps appear to be older than most craters in the transition zone, though some relations are ambiguous. The mountain ranges of the transition zone are thought to be the products of block faulting, with some rotation. The faulting that produced the transition zone structures very probably occurred contemporaneously with the formation of the Hellas basin. The process would have been relatively rapid in the impact model, as it results from the gravitational collapse of the surrounding area toward the deep initial crater along normal faults, producing ring structures. The faults may have been subsequently rejuvenated. If the basin was formed by tectonic subsidence, the faulting may have occurred in stages separated by substantial periods of time.

Preliminary data indicate that there is a very slight negative free-air gravity anomaly over Hellas relative to the area west of Hellespontus Montes, (Lorell and others, 1973). The anomaly is roughly equivalent to a 1 km topographic depression in a spheroid, whereas the basin floor actually lies as much as 8 km below the adjacent area of Hellespontus Montes, according to radio occultation data (Kliore and others, 1972). The gravity figures imply that there is a mass concentration beneath Hellas dense enough to compensate for all but 1 km of the actual topographic depression. The negative gravity anomaly implies that the Hellas basin should tend to rise isostatically, arguing against a tectonic subsidence model. These conclusions are speculative since both gravity and topographic data are imprecise in this area.

Many workers, including Masursky (1973), Wilhelms (1973), Potter (1976) and others, have interpreted the Hellas basin as an impact feature. This interpretation appears valid although tectonic subsidence cannot be totally ruled out on the basis of present knowledge. A volcanic origin is considered unreasonable because of the size of the feature compared with terrestrial volcanic features. An impact origin is favored for several reasons: (1) numerous asteroids, and perhaps large comets, are massive enough to have created the Hellas basin by impact; (2) similar large basins are found on three bodies of substantially different internal composition and structure (Mars, the Moon, and Mercury), indicating an exogenous basin-forming process; and (3) a relatively low-velocity impact of a dense planetesimal might account for the mass concentration that apparently exists under Hellas. The apparent age of the Hellas basin (early c_1 or pre-c_1 crater time if created by impact) implies that it may have been formed by the impact of a planetesimal left over from the major accretional stage of Mars.

A marked regional trend of linear ridges, scarps, and troughs concentric about Hellas was previously noted by Scott and others (1972); Binder and McCarthy (1972); and Schultz and Ingerson (1973), who noted that the dominance of concentric linear features about Hellas is similar to that about the oldest lunar basins, where concentric structures persist or are rejuvenated but where radial ejecta patterns have been degraded with age. This is further evidence that the Hellas basin is very old.

The three rings shown were derived from major structural features concentric about the center of the Hellas basin (at about 40° S, 292° W). The long, low ridge trending NNW at 53° S, 353.5° W., could be related to an additional ring. The mountain ranges at 33° S, 335° W and at 35° S, 336.2° W. appear to be directly related to the long northeast-trending scarps immediately to the east of the ranges. These scarps are probably fault scarps and are interpreted to be the margins of a major graben or rift valley. The entire system is concentric about Hellas and represents part of the third ring structure.

MOUNTAINS

Individual mountains probably have different origins, but a general interpretation is that most of them are peaks of older material protruding through younger layers. Many of them could be volcanoes. It is thought that few, if any, are ejecta blocks. The range at 63.5° S., 342° W., has a distinct linear grain trending about N 20° E.

VOLCANISM

A variety of probable volcanic features is found in the quadrangle. In the southeastern part, three ancient calderas are located at the summit of a sprawling shield complex more than 1,300 km long (referred to as the Amphitrites Patera shield complex). Several calderas lie immediately east in the Hellas quadrangle. The marginal contacts of this shield complex are commonly indistinct in available imagery; a rough estimate of its area is 10^6 km². The Amphitrites Patera shield complex apparently rises less than 5 km above the adjacent Hellas basin floor and much less over the high cratered plain to the west (Barth and others, 1974); most of its volume is probably on the basin side, and it buries transition zone structures. The vast area and gentle slopes of the shield complex suggest a low-viscosity basaltic composition for its lavas but are mainly attributed to the coalescence of several individual shields, each erupted from a separate vent. The higher density of impact craters on the Amphitrites Patera shield complex relative to the shields of the Tharsis region indicates that it is older; isostatic adjustment may be in part responsible for its gentler slopes. Potter (1976) suggested that the Amphitrites Patera shield complex and Hadriaca Patera, a smaller shield on the northeast rim of the Hellas basin, may be only thin veneers of lava. The calderas of both of these shields are located over the old rim of the basin and it is apparent that the volcanic activity was influenced by the transition zone fractures. Potter (1976) suggested that these shields may be located at the intersection of the basin rim with a major northeast-trending fracture system. The crater Barnard (at 61° S., 300° W.) is interpreted as an impact crater modified by volcanism; Potter (1976) considered it a fresh caldera.

To the southwest, the shield complex appears to be overlain by ridged plains material. The ridged plains are interpreted to be composed of flood lavas (probably of basaltic composition considering their areal extent) because of the presence of: (1) many wrinkle ridges, thought to be volcanic extrusions along fissure systems that may indicate the locations of feeder dikes for flood lavas; (2) an associated probable volcanic center just south of the quadrangle at 67° S., 323° W.; (3) several dozen probable cinder cones (West, 1974; Peterson, 1974); and (4) cratered domes in many impact craters found in the ridged plains. The cratered domes occur at the centers of craters more than 32 km in diameter, whereas smaller craters have central peaks. It is thought that the >32 km craters penetrated to a depth sufficient to either trigger local volcanism or release already molten material at depth whereas the <32 km craters did not. Many of the craters within and surrounded by the ridged plains were apparently partly filled by ridged plains lavas extruded from below at some later time when pressure was insufficient to produce a dome structure.

Australis Tholus (at 57.5° S., 322° W.) looks like a cratered dome, but unlike the other cratered domes, is not located within a crater and may have had a different origin; however, it is probably also a small shield.

A number of small domes, up to 18 km across, were mapped within the area of ridged plains. They do not occur in craters and lack detectable summit pits. Of uncertain origin, they could be volcanic domes and/or erosional mesas.

Two prominent peaks on the floor of Hellas were mapped as cratered mountains. One appears to be fresh, the other eroded. The fresh cratered mountain has a basal diameter of 11 km, a 3-km-wide summit crater, and a slope of about 22° (determined from shadow measurements), dimensions reasonable for a stratovolcano. The cratered mountains and the apparent cinder cones of the ridged plains (similar in size and form to terrestrial cinder cones such as those of the San Francisco Volcanic Field in Arizona) are evidence for pyroclastic material, contrary to the conclusion of Carr (1973) that Mars lacks evidence of explosive volcanism.

REGIONAL UNITS

Age determinations of regional units (such as rugged material and ridged plains material) were based partly on density distributions of impact craters more than 10 km in diameter and partly on stratigraphic relations such as superposition and embayment. The density distribution of smaller craters was not considered because of the strong and varied effects of the debris mantle and poor quality of imagery.

Unconsolidated fine surficial sediments forming the debris mantle discussed by Soderblom and others, (1973) cover most of the quadrangle and are thought to make up at least the upper parts of plains material, peripheral basin-floor material, and central basin-floor material. Lower parts, at depths of the order of metres or tens of metres, may be coarser unconsolidated material like lower parts of the lunar regolith.

Plains material apparently varies in thickness locally, generally thinning toward the north. Crater densities show the subjacent bedrock to be very old; possible flow fronts seen in B-frames suggest that it may consist of flood lavas in some places. Some B-frames show subunits of plains material such as pitted plains and lineated plains not mappable from A-frames.

The cause of the apparent difference in elevation of central basin-floor material and peripheral basin-floor material remains undetermined, but could be a function of isostasy. Topographic mapping in Hellas is unreliable and the generalized contours do not indicate the apparent higher elevation of central basin-floor material relative to peripheral basin-floor material. Some major structures, including a 35-km diameter crater, are visible in the central basin-floor material and may be exhumed features of the subjacent bedrock or degraded structures in the central basin-floor material itself. Peripheral basin-floor material is thought to be derived from both the transition zone and central basin-floor material. Here, as elsewhere on Mars, wind is probably the primary agent of erosion and deposition, although running water may have played a role at times in the past, perhaps periodically.

The rugged material around the 200-km crater Kaiser, centered near 47° S., 340° W., is thought to be genetically related to the crater and may be fractured bedrock exposed by the erosion of ejecta. Other outcrops that form rugged terrain are similarly interpreted as exposed bedrock. Rugged terrain is very old according to crater densities and probably much more extensive than shown, but buried under other units. Outcrops may be more extensive but masked by atmospheric haze in the pictures. The same is true of hummocky terrain. More accurate mapping of regional units will require new imagery with less atmospheric obscuration.

CHANNELS

The depressions mapped as channels (near 31° S., 335° W.) are thought to be fluvial in origin, on the basis of two observations: (1) the channels are joined together in a dendritic tributary system with the various branches merging in the downslope direction (SE to NW as indicated by a scarp cut by a main channel), and (2) they become broader and deeper in the downslope direction. These characteristics are typical of fluvial channels but not of lava channels. The channel locations may have been controlled by a joint or fault system. This channel system is not related to any visible surface source and seems to require an atmospheric source of water, which would imply a radically different climate in the past. The apparent sparcity of channels elsewhere in the quadrangle is thought to be due to burial by surficial sediments and to a lack of haze-free imagery, not to an actual lack of channels (D. C. Pieri, 1974, oral commun.). Isolated sinuous depressions visible in some pictures were mapped as troughs because none of them are joined in networks and other channel characteristics are not detectable.

EOLIAN FEATURES

There is extensive evidence of eolian activity within the quadrangle. Numerous dark streaks, invariably related to topographic features, are indicative of recent prevailing wind directions. One dark splotch, on the floor of the crater Proctor (at 48° S., 330° W.), has proved to be a dune field in B-frames (Cutts and Smith, 1973; Peterson, 1974); by analogy, other similar splotches in the vicinity are interpreted to be dune fields. However, dark splotches are probably not all alike. Long, narrow, filamentlike dark streaks are common, as are cuspate interfaces between light and dark material. Bright streaks common in other areas on Mars are not observed within the quadrangle.

Dark streaks and splotches may be formed by the erosion or nondeposition of bright material over dark material, or by the trapping of dark sediments. Some are interpreted to be superficial depositional features because they appear to be draped over the local topography. Some splotches lap over crater walls and extend downwind as streaks. Dark splotches in the southwestern part of the quadrangle occur both in craters and on the intercrater plains and are irregular in outline. Some of the intercrater dark splotches were observed to change markedly in size and form in a few weeks time (Sagan and others, 1972). Those of the central part of the quadrangle tend to be more regular (generally oval) in outline, occur on the floors of craters, and seem to be relatively stable.

Erosional features such as deflation hollows and yardangs may exist, as noted in several B-frames. Pedestal craters are apparently produced by differential eolian erosion, the pedestals surviving owing to the armoring effect of coarse ejecta protecting subjacent fine material.

The great Hellas basin, frequently the site of intense local dust storms, is undoubtedly a major trap for fine sediments, though big storms may remove material from the basin. Many small craters throughout the quadrangle are sediment traps, being in some places completely filled by fine material. The Hellas basin fines and the fines of the debris mantle probably are the main components of the periodic global dust storms. Arvidson (1974) noted that these storms usually begin around the west margin of Hellas.

GEOLOGIC HISTORY

In the late stages of the accretion of Mars, the basin in the northwest part of the quadrangle was formed by the impact of a large body. Intense cratering (pre-c_1 or early c_1) continued throughout the region, and probably over the entire planet. The Hellas basin was formed by a tremendous impact in early c_1 crater time. Ejecta from the impact probably covered the entire quadrangle and may have formed some of the mountains and the hummocky terrain now exposed. The structural rings of Hellas, including transition zone features, were formed very soon after the impact. Intense cratering continued, obliterating most of the Hellas ejecta and radial sculpture. Extensive erosion of the cratered terrain further subdued the Hellas ejecta and radial sculpture, leaving remnant mountains and high areas of hummocky terrain. Intense cratering continued through the time of c_2 crater formation, when flood lavas were probably extruded over vast areas, then declined. The filling of the basin near 37.5° S, 356° W, which probably began much earlier, was completed. The volcanic shield complex in the southeast, which may have been active much earlier and for a long period of time, became extinct. The flood lavas of the ridged plains were extruded, probably in late c_2 and early c_3 crater time. Sporadic cratering continued, but not nearly as intensively as in c_1 and c_2 crater time. The surficial sediments forming the bulk of the plains material and Hellas floor material may have been deposited during c_3 and c_4 crater time although deposition and reworking of sediments probably began much earlier. The cinder cones found in the southern area of ridged plains material were formed in c_4 crater time after considerable reworking of the local surficial sediments. Sparse impact-cratering activity has probably continued to the present time. Rejuvenation of transition zone faults may have occurred occasionally since their initial formation. Fluvial activity appears to have been episodic at least in relatively recent Martian geologic time. There has probably been constant eolian activity since the atmosphere of Mars first formed, producing both erosional and depositional features; however, the effectiveness of eolian activity may have varied episodically with major climatic changes.

REFERENCES

Arvidson, R. E., 1974, Wind-blown streaks, splotches, and associated craters on Mars—Statistical analysis of Mariner 9 photographs: Icarus, v. 21, p. 12-27.
Barth, C. A., Hord, C. W., Stewart, A. I., Lane, A. L., Dick, M. L., Schaffner, S. H., and Simmons, K. E., 1974, Mariner 9 Mars orbiter ultraviolet spectrometer experiment—An Atlas of Mars: Local Topography: Colorado Univ., Boulder, Laboratory for Atmospheric and Space Physics, 739 p.
Binder, A. B., and McCarthy, D. W., Jr., 1972, Mars: The lineament systems: Science, v. 176, p. 279-281.
Carr, M. H., 1973, Volcanism on Mars: Jour. Geophys. Research, v. 78, p. 4049-4062.
Cutts, J. A., and Smith, R. S. U., 1973, Eolian deposits and dunes on Mars: Jour. Geophys. Research, v. 78, p. 4139-4154.
Kliore, A. J., Cain, D. L., Fjeldbo, G., Seidel, B. L., Sykes, M. J., and Rasool, S. I., 1972, The atmosphere of Mars from Mariner 9 radio occultation measurements: Icarus, v. 17, p. 484-516.
Lorell, J., Born, G. H., Christensen, E. J., Esposito, P. B., Jordan, J. F., Laing, P. A., Sjogren, W. L., Wong, S. K., Reasenberg, R. D., Shapiro, I. I., and Slater, G. L., 1973, Gravity field of Mars from Mariner 9 tracking data: Icarus, v. 18, p. 304-314.
Masursky, Harold, 1973, An overview of geological results from Mariner 9: Jour. Geophys. Research, v. 78, p. 4009-4030.
McCauley, J. F., Carr, M. H., Cutts, J. A., Hartmann, W. K., Masursky, Harold, Milton, D. J., Sharp, R. P., and Wilhelms, D. E., 1972, Preliminary Mariner 9 report on the geology of Mars: Icarus, v. 17, p. 289-327.
Peterson, J. E., 1974, Geology of the Noachis quadrangle, Mars: Colorado Univ., Boulder, Ph. D. thesis, 165 p.
Potter, D. B., 1976, Geologic map of the Hellas quadrangle of Mars: U.S. Geol. Survey Misc. Geol. Inv. Map I-941.
Sagan, Carl, Veverka, Joseph, Fox, P., Dubisch, R., Lederberg, J., Levinthal, E. C., Quam, Lynn, Tucker, Robert, Pollack, J. B., and Smith, B. A., 1972, Variable features on Mars: Preliminary Mariner 9 television results: Icarus, v. 17, p. 346-372.
Schultz, P. H., and Ingerson, F. E., 1973, Martian lineaments from Mariner 6 and 7 images: Jour. Geophys. Research, v. 78, p. 8415-8427.
Scott, D. H., Peterson, J. E., and Wilhelms, D. E., 1972, Prototype and preliminary geologic mapping of Mars from Mariner 6 and 7 data, part 2: Preliminary small-scale regional mapping (1:5,000,000): U.S. Geol. Survey Interagency Report; Astrogeology 45, p. 11-17.
Soderblom, L. A., Kreidler, T. J., and Masursky, Harold, 1973, Latitudinal distribution of a debris mantle on the Martian surface: Jour. Geophys. Research, v. 78, p. 4117-4122.
West, M. N., 1974, Martian volcanism: Additional observations and evidence for pyroclastic activity: Icarus, v. 21, p. 1-11.
Wilhelms, D. E., 1973, Comparison of Martian and Lunar multiringed circular basins: Jour. Geophys. Research, v. 78, p. 4084-4095.

For sale by Branch of Distribution, U.S. Geological Survey,
1200 South Eads Street, Arlington, VA 22202, and Branch of Distribution,
U.S. Geological Survey, Box 25286, Federal Center, Denver, CO 80225.